J Comput Aided Mol Des (2006) 20:735–749
DOI 10.1007/s10822-006-9086-7

ORIGINAL PAPER

Incorporating partial matches within multiobjective pharmacophore identification

Simon J. Cottrell · Valerie J. Gillet · Robin Taylor

Received: 6 June 2006 / Accepted: 13 October 2006 / Published online: 4 January 2007

Abstract This paper describes the extension of our earlier multiobjective method for generating plausible pharmacophore hypotheses to incorporate partial matches. Diverse sets of molecules rarely adopt exactly the same binding mode, and so allowing the identification of partial matches allows our program to be applied to larger and more diverse datasets. The method explores the conformational space of a series of ligands simultaneously with their alignment using a multiobjective genetic algorithm (MOGA). The principles of Pareto ranking are used to evolve a diverse set of pharmacophore hypotheses that are optimised on conformational energy of the ligands, the goodness of the overlay and the volume of the overlay. A partial match is defined as a pharmacophoric feature that is present in at least two, but not all, of the ligands in the set. The number of ligands that map to a given pharmacophore point is taken into account when evaluating an overlay. The method is applied to a number of test cases extracted from the Protein Data Bank (PDB) where the true overlay is known.

S. J. Cottrell · V. J. Gillet (✉)
Department of Information Studies, University of Sheffield,
Regent Court, 211 Portobello Street, Sheffield S1 4DP, UK
e-mail: v.gillet@sheffield.ac.uk

R. Taylor
Cambridge Crystallographic Data Centre, 12 Union Road,
Cambridge CB2 1EZ, UK

Present Address:
S. J. Cottrell
Institut für Pharmazeutische Chemie, Philipps-Universität
Marburg, Marbacher Weg 6, 35032 Marburg, Germany

Keywords Pharmacophore · Molecular alignment · MOGA · Multiobjective optimisation · Multiobjective genetic algorithm · Partial matches

Introduction

A pharmacophore describes the spatial arrangement of chemical features required for a small molecule to bind to a receptor. Pharmacophore identification methods are usually applied to a series of molecules known to bind to a receptor, when the three-dimensional structure of the receptor is unknown. The first generation of pharmacophore identification programs have been around for more than a decade [1–4]. However, recently some of the limitations of these early methods have been highlighted [5, 6] and several new approaches are now beginning to appear that address some of these limitations [7–10].

Pharmacophore identification involves identifying common pharmacophoric features within the molecules, that is, atoms or functional groups that can interact with a receptor in a similar way, and then aligning the bioactive conformations of the molecules such that their corresponding features are overlaid. The bioactive conformations of the molecules are not usually known and so some form of conformational analysis is usually carried out. For many datasets, there are numerous plausible ways of overlaying the molecules, due to the presence of multiple features within the molecules and due to the multiple accessible conformers that may exist for each molecule. In such cases, it is important that the chemist is presented with a range of alternative hypotheses that can be validated further, for example, by database searching or by the synthesis of new compounds.

The quality of a pharmacophore hypothesis is usually judged on a number of criteria. For example, the GASP program [2] evaluates a pharmacophore on the number of pharmacophoric points it consists of, the quality of the mapping of each molecule onto the pharmacophore (which includes consideration of site points together with their associated heavy atoms), the common volume of the overlaid molecules and their conformational energy. GASP is based on a traditional optimisation technique in which the multiple criteria are combined into a single weighted-sum fitness function. Specifically, the fitness function in GASP combines three components that take account of the feature alignment, the volume overlap and the conformational energy. This approach reduces the problem to a single-objective optimisation problem that can be handled by a single-objective optimisation method, such as the genetic algorithm (GA) in GASP.

There are, however, a number of limitations with traditional optimisation methods. Typically the objectives are in competition with one another so that a better alignment (as measured by the volume score, for example) can be achieved by conformers that are strained away from their minimum energy conformations. Thus, a trade-off usually exists in the criteria to be optimised. In the traditional approach, this is handled through the use of relative weights which determine the relative importance given to the individual objectives and the particular compromise solution that is sought. However, it can be difficult to assign appropriate weights, especially when the criteria are non-commensurate, as is the case here. Default weights in GASP were defined empirically by analysing a relatively small number of test cases. However, there is no reason to assume that a set of weights that is relevant for one particular test case will also be relevant for another. Furthermore, the result of a single-objective optimisation is a single solution that maximises (or minimises) the function, yet in the absence of the receptor itself, it is unlikely to be possible to predict unambiguously how to overlay a series of ligands known to bind to the receptor.

In a previous study, we have explored the use of a multiobjective optimisation method which aims to find a diverse set of pharmacophore hypotheses that are all plausible for a given set of ligands [9]. The algorithm explores the conformational space of the ligands simultaneously with their alignment. The same objectives as in GASP are calculated, but they are treated independently without the need to define relative weights. The method is based on the Pareto principles of multiobjective optimisation [11, 12]. According to these principles, a solution is defined as *Pareto-optimal* if none of the individual objectives can be improved without worsening another objective. A representative set of such solutions can then be extracted, chosen so that they include a diverse range of individual objective values and molecular alignments. Our method was shown to be successful in identifying hypotheses that are very similar to previously published hypotheses, for test cases where the best solution identified by the weighted-sum method in GASP was incorrect. To our knowledge, Pareto ranking was first applied in the field of Chemoinformatics by Handschuh et al. for the flexible superposition of 3D structures [13]. The differences between this first approach and our work are described in our previous paper. More recently multiobjective optimisation methods have also been applied to combinatorial library design [14], derivation of quantitative structure activity relationships [15] and to the de novo design of molecules [16]. Multiobjective optimisation techniques have also been applied to pharmacophore identification in the GALAHAD program; the full details of this method are not yet published; however, the underlying approach appears to be quite different to that described here [10].

In our previous work [9] we were able to demonstrate the benefits of the multiobjective optimisation approach over a traditional GA, however, we also highlighted a limitation in the method which also applies to GASP. This is the restriction that each pharmacophore point generated must be mapped to a feature in every ligand. This effectively limits both programs to handling very small numbers of carefully chosen compounds [5]. In this paper, we build on the previous work by increasing the functionality of the multiobjective optimisation approach to allow partial matches to be identified for a series of ligands. Other programs exist that can find overlays involving partial feature matches (e.g. Catalyst HipHop [17]), but we believe our algorithm to be a novel method of incorporating partial matching into a multiobjective pharmacophore search program. The result is to widen the search so that solutions containing partial matches are automatically considered alongside more restricted solutions, with no necessity for any user input.

Implementation of partial matches has required significant changes to be made to the chromosome representation, the alignment method and to the feature score so that full matches are distinguished from partial matches. Allowing partial matches to be identified increases the search space to be explored significantly and so we have introduced the use of distance constraints which can be used to improve both the efficiency and the effectiveness of the algorithm. We have also extended the definition of hydrophobes to include aliphatic rings and to allow user-defined hydrophobic features. Taken together, these enhancements allow increased numbers of more diverse molecules to be handled. The method has been applied to sets of ligands extracted from the Protein Data Bank (PDB) [18] where the true pharmacophores are known. Examples have been chosen where partial matches are known to exist and the new methodology is validated on the ability of the multiobjective genetic algorithm (MOGA) to identify ligand overlays that are close to those obtained by least-squares superposition of the corresponding experimental protein–ligand structures. However, it should be noted that in all cases a range of different hypotheses are found.

Method

We have extended the MOGA described previously [9] to allow the pharmacophore hypotheses identified to include partial matches. A partial match is defined as a pharmacophoric feature that is present in at least two, but not all, of the ligands in the set. The algorithm is described in detail below, with particular emphasis given to the new methodology.

The ligands are input to the program as energy minimised conformations. The first step is to identify the pharmacophoric features within each ligand. Donor and acceptor features are defined as in GASP, however, the definition of a hydrophobe has been extended to include aliphatic rings and user-defined groups, in addition to the aromatic rings defined previously. Each hydrophobic ring is represented by a virtual point created at the centre of the ring and a normal to the ring. A user-defined hydrophobe, such as a *t*-butyl group, is specified as a list of atoms and a virtual point is created at the centroid of the atoms. Donors and acceptors are represented by virtual points that correspond to the hypothetical positions of acceptors or donors in the receptor binding site. Thus, a virtual point is created at 2.9 Å from the heavy atom attached to each hydrogen-bond donor proton and at 2.9 Å from the heavy atom associated with each acceptor lone pair.

Encoding conformation

The chromosome consists of a conformational part and a mapping part which is described below. The conformational part consists of a set of *N* strings to represent the conformation of each of the *N* ligands. Each rotatable bond in each ligand is encoded as an 8-bit number, which gives a resolution of about 1.4°. This encoding of conformation is unchanged from our previous work [9].

Encoding partial mappings

The mapping part of the chromosome has been modified substantially from that described previously [9] to encode both full and partial mappings in a mapping table. The mapping table consists of one row per molecule with each column representing a potential pharmacophore point of a particular type. The cells in a column represent the features in each molecule that are mapped to the corresponding pharmacophore point. The number of columns of each feature type is user-defined and need not be larger than the maximum number of features of that type in any molecule in the set. If set to a smaller value, the search space is reduced—making it more tractable—but there is a risk that the reduced search space might not contain the true solution. Partial mappings are encoded through the use of *dummy* features which are added to the *real* features in each molecule. Like real features, they are of a specific type, i.e. donor, acceptor or hydrophobe. Each cell of the mapping table may contain either a real or a dummy feature of the relevant molecule. Thus, the number of molecules which have a real feature contained within a given column may vary between zero and the number of molecules in the dataset. A mapping column that contains real features in fewer than two molecules has no physical significance. Thus, the number of real mappings may vary depending on how many columns contain real features in at least two molecules.

A mapping table is illustrated in Fig. 1 for a hypothetical set of molecules that bind at the same (hypothetical) site but form different and overlapping sets of interactions. The most plausible way of overlaying the molecules is shown and a hypothetical chromosome that would lead to this alignment is shown in Table 1. Note that only the mapping part of the chromosome is shown; it is assumed that the conformational part contains appropriate torsion angles. The chromosome refers to the features of each molecule using the labels assigned to them in Fig. 1.

There are three mapping columns for each feature type. The first donor column represents a donor formed by H_1 in molecule **1** and H_1 in molecule **2**. Molecules **3** and **4** do not have features that map to this pharmacophore point, as represented by the dummy features. The second donor column represents a donor that is mapped to a feature in every molecule

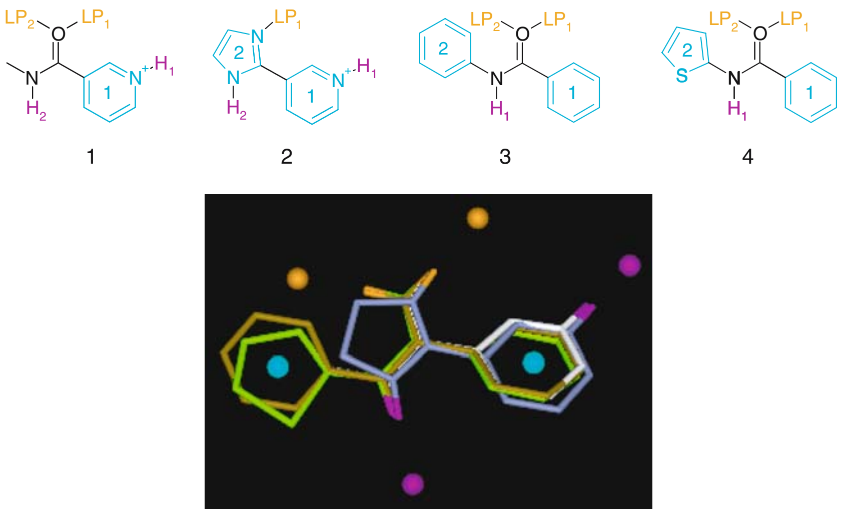

Fig. 1 An overlay of hypothetical molecules **1**–**4** that corresponds to the mapping shown in Table 1. **1** is white, **2** is blue, **3** is brown and **4** is green. The donors are shown in purple and acceptors in orange. The hydrophobic groups are not highlighted to ease distinction of the molecules

Table 1 A mapping table that leads to the overlay in Fig. 1

	Donors (H)			**Acceptors (LP)**			**Hydrophobes**		
Molecule 1	1	2	Du	1	2	Du	1	Du	Du
Molecule 2	1	2	Du	1	Du	Du	1	Du	2
Molecule 3	Du	1	Du	1	2	Du	1	2	Du
Molecule 4	Du	1	Du	1	2	Du	1	2	Du

The number of columns of each type is user-defined. The integers in the columns refer to the subscript labels used to identify donors and acceptors and to the ring labels used to identify the hydrophobes. "Du" indicates a dummy feature. Dark shading indicates mappings involving all molecules. Light shaded columns indicate partial mappings and the unshaded columns involve fewer than two molecules and do not represent real mappings

(specifically H_2 in **1**, H_2 in **2**, H_1 in **3** and H_1 in **4**). The third donor column is not mapped to a real feature in any of the molecules and hence does not represent a pharmacophore point.

The population of chromosomes is initialised by making random assignments of molecule features (real and dummy) in the mapping table and by assigning torsion angles at random. The genetic operators of crossover and mutation are applied to the chromosomes in order to generate child chromosomes. Dummy features are treated in the same way as real features by the genetic operators; however, they are not used in the alignment procedure which is described below.

Generating an alignment

The information encoded in the chromosome is used to generate an alignment of the molecules prior to evaluation of the fitness of the chromosome. First, a conformation is generated for each molecule by applying the appropriate bond rotations encoded in the conformation part of the chromosome. The alignment is then built incrementally using the mapping table and a "framework" method that is similar to that described by Sutcliffe et al. for the alignment of protein sequences [19] but has been adapted to allow for partial mappings. Consider a mapping table consisting of n rows (molecules) and m columns (potential pharmacophore features). Molecule k, represented in the mapping table by a row consisting of m features, P_{k1} to P_{km}, (each of which may represent a real feature or a dummy), is fitted to a framework which has been derived from the mappings of molecules 1,...,k – 1. In the description below, framework $^{k}\mathbf{F}$ refers to the framework that has been derived from molecules 1,...,k. The framework data structure consists of m points, each related to one of the mapping columns in the chromosome. Each point represents a potential pharmacophore point, derived from real features in the related mapping column, or it may be null, if the column consists entirely of dummy features for molecules 1,...,k. The point in $^{k}\mathbf{F}$ related to mapping column a shall be denoted $^{k}F_{a}$.

The framework is initialised with the first molecule. For each mapping column a that maps to a real feature in molecule **1**, ${}^{1}F_a$ is set to the co-ordinates of feature P_{1a}. For each column that maps to a dummy feature, ${}^{1}F_a$ is a null point. Then, for each subsequent molecule i, where $1 < i \leq n$, framework ${}^{i}\mathbf{F}$ is calculated by least-squares fitting of molecule i to framework ${}^{i-1}\mathbf{F}$ as follows.

For each mapping a:

(i) If ${}^{i-1}F_a$ is null and P_{ia} is a dummy feature, ${}^{i}F_a$ is null.

(ii) If ${}^{i-1}F_a$ is non-null and P_{ia} is a dummy feature, ${}^{i}F_a$ is set equal to ${}^{i-1}F_a$.

(iii) If ${}^{i-1}F_a$ is null and P_{ia} is a real feature, ${}^{i}F_a$ is set equal to the co-ordinates of P_{ia}.

(iv) If ${}^{i-1}F_a$ is non-null and P_{ia} is a real feature, ${}^{i}F_a$ becomes the weighted centroid of ${}^{i-1}F_a$ and the co-ordinates of P_{ia}. The calculation is weighted towards ${}^{i-1}F_a$ in the ratio $r({}^{i-1}F_a)$:1 where $r({}^{i-1}F_a)$ is the number of real features which mapping a maps in molecules 1,...,i–1, i.e. the number of points from which ${}^{i-1}F_a$ was derived.

Only in case (iv) does mapping a represent an actual mapping between molecule i and the preceding molecules. Therefore the least-squares fitting between framework ${}^{i-1}\mathbf{F}$ and molecule i is restricted to the mappings falling into case (iv) and it can only be performed if the mapping involves at least three points. Any chromosome which does not contain at least three real mappings in every molecule is rejected. The least-squares fitting is based on the Kabsch algorithm [20].

The sequential alignment of the molecules to a common framework results in the framework being adjusted at each step to reflect all the molecules incorporated thus far. However, the alignment that is generated is dependent on the order in which the molecules are specified in the configuration file. Specifically, while the mapping of molecule k does influence the alignment of any molecule l, where $l > k$, it cannot influence the alignment of molecules i and j relative to each other, where $i, j < k$. In Sutcliffe's approach, a particular molecule is chosen at random for the initial alignment; however, the bias caused by this is minimised by iteratively refining the alignment until the variation in the framework from one iteration to the next is less than a specified threshold. This has not been implemented here and development of an order-independent method is currently being investigated.

Fitness calculation

Once an alignment has been generated, it is then possible to calculate the objective scores for the solution. Our method uses three objectives: a feature objective, a volume objective, and an energy objective.

The feature score is based on that implemented previously but has been adapted here to reflect partial mappings in the pharmacophore. Thus, it takes into account the number of pharmacophoric points, the number of molecules that are mapped to each pharmacophore point and the quality of the overlay. Firstly, a pharmacophore point only contributes to the score if the mapped features are overlaid sufficiently closely. Thus, even though a set of features may be mapped in the chromosome, if it is not possible to overlay them closely they do not contribute to the feature score. For each valid pharmacophore point, a score that is a function of the RMSD between the features involved in the mapping and their centroid is calculated. This score takes into account the overlay of both the heavy atoms and the virtual points for hydrogen-bonding features, and both the overlay of the ring centroids and the alignment of the ring normals for the hydrophobic features, as described in Jones et al. [2] Hence, pharmacophore points that are formed from closely aligned features make a larger contribution to the features score than ones resulting from features that are poorly aligned. A weighting factor of 2^{m-n} is then applied, where there are m molecules in the mapping and n is the number of molecules in the dataset. Thus, a mapping that excludes one molecule from a set of four would have a weight of 1/2, a mapping that excludes two molecules would have a weight of 1/4, and so on. Thus, more weight is given to features that are common to the entire dataset and which are therefore less likely to have arisen by chance, than to features which are found in only a subset of the dataset. Furthermore, the weighting scheme ensures that a mapping involving all of the molecules scores more highly than two mappings which each consist of a subset of the molecules, assuming that the qualities of the alignments are similar.

The volume and energy scores are calculated as described previously and are described here in brief. The volume objective score is defined as the mean overlap between the first molecule and each of the other molecules. Each atom is considered as a hard sphere whose radius is the van der Waals radius for the atom type as defined in the Tripos 5.2 force field. The volume overlap between two molecules is a sum of the hard-sphere overlap for each pair of atoms between the two molecules, and is calculated using a simple geometric formula. As for the alignment procedure, the volume score is biased by the order in which the molecules are specified. The energy score is the mean of the internal van der Waals energy calculated for each molecule. It is the only one of the three objectives which is independent of the alignment of the molecules. The energy of each molecule is a sum of the energy calculated for each pair of atoms within the molecule, using a Lennard–Jones 6–12 potential based on the Tripos 5.2 force field.

Once the three objective scores have been calculated for each solution, Pareto ranking is applied to the population. One solution is said to *dominate* another solution if it is better in all three objectives. (For the feature and volume objectives, the aim is to maximise the scores, while for the energy objective the aim is to minimise the score). The Pareto rank of each solution is the number of other solutions in the population by which it is dominated. Thus, the best solutions are those which are not dominated by any other solutions and hence have a rank of zero.

Evolution of the population

The population evolves by application of the crossover and mutation genetic operators. The parent chromosomes for these operators are chosen by roulette-wheel selection [11], with selection biased towards individuals of lower rank. However, since a potentially infinite number of solutions can exist on the Pareto surface it is necessary to include a niching strategy to ensure that a diverse set of solutions is found. Maintaining diversity in a MOGA is often achieved through the use of objective space niching, whereby individuals that are in crowded regions of the search space are penalised relative to those in sparsely populated regions. However, this strategy did not prove effective in this application, as described previously [9], due to the weak correspondence between diversity in objective space and diversity in the pharmacophores represented by the individual solutions. Therefore, an alternative mapping-based niching scheme was employed which has been modified here to account for partial mappings.

The first step is to cluster the individuals based on the mappings they represent. The clustering step considers mappings that involve all of the molecules and does not take into account differences in partial mappings. This is because differences in the partial mappings usually only reflect small variations to the alignment of local regions of the molecules with the overall alignments being similar. Furthermore, the clustering compares all permutations of one mapping with another since there is no order imposed on the columns included in the mapping table. The probabilities of selecting the chromosomes for reproduction are adjusted as shown schematically in Fig. 2.

Distance constraints

Allowing partial mappings to exist within a pharmacophore greatly increases the size of the search space,

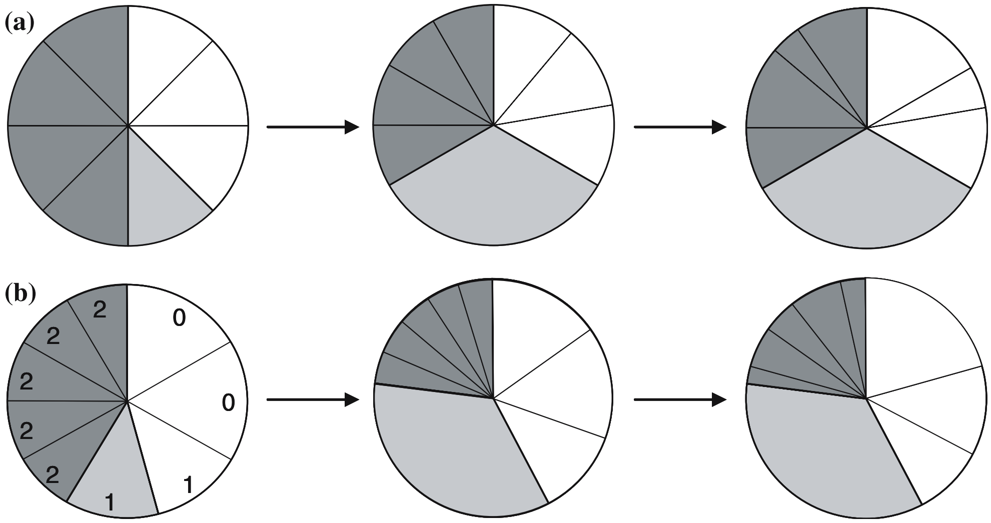

Fig. 2 ‘‘Roulette-wheel’’ segments for two hypothetical MOGA populations, each containing three distinct feature mappings or clusters (shown in different shades). (**a**) Each individual is non-dominated, and so, initially, has an equal probability of being chosen (left). After adjusting for the number of individuals in each cluster, there is an equal probability of choosing a chromosome from each cluster (centre). (**b**) Some individuals are dominated with the rank of each chromosome as shown (left). If two clusters have the same density, the one containing individuals of lower mean rank is more likely to be chosen. The relative probabilities of selecting the different individuals within each cluster remain the same (centre). In both cases, the probabilities are then further adjusted through objective-space niching, but keeping the overall probability of selecting an individual from each cluster the same (right)

compared to the more restrictive case when all features must be present in all molecules. Although the aim of the partial matching methodology is to increase the size and diversity of the datasets that can be handled, in practice, the greatly enlarged search space limits the number of molecules that can be handled, especially when the molecules are feature rich. However, a significant reduction in the search space can be achieved through the use of distance constraints which can be used to eliminate solutions containing geometrically infeasible mappings from the population.

For example, consider the two CDK2 inhibitors in Fig. 3. The donor arising from the sulphonamide group and acceptor highlighted in **5** are constrained to lie much further apart than the highlighted donor and acceptor in **6** (for which there is no flexibility at all), and it is therefore not possible to overlay both sets of mapped features simultaneously. Upper and lower bounds on the distance between each pair of features within each molecule can be calculated, for example, using distance geometry techniques [21]. A chromosome is rejected if it contains a mapping between feature $X1$ and $X2$ in molecule X and feature $Y1$ and $Y2$, respectively, in molecule Y and:

$$\begin{aligned}&\min\left(d_{X1,X2}\right) > \max\left(d_{Y1,Y2}\right) + \mathrm{TOLERANCE}\\ \text{or } &\max\left(d_{X1,X2}\right) < \min\left(d_{Y1,Y2}\right) - \mathrm{TOLERANCE}\end{aligned}$$

where $d_{X1,X2}$ is the intramolecular distance between $X1$ and $X2$, etc. and the TOLERANCE is set to 2.0 Å.

Results

The partial match methodology has been applied to two sets of ligands extracted from the PDB [18]. The ligands were extracted from their respective complexes and energy minimised using the Tripos 5.2 force field with Gasteiger–Marsili charges assigned. The MOGA was then used to identify plausible pharmacophores. In the following experiments, all five- and six-membered rings were identified as possible hydrophobic features. Unless otherwise stated, the runs were performed on a 2.8 GHz Linux PC using the parameters shown in Table 2. The number of operations and the number of mapping columns in the chromosome varied between experiments and are specified in the details of each experiment.

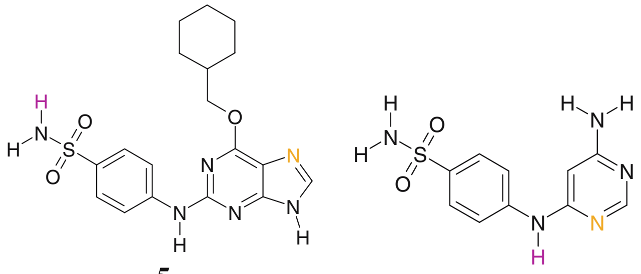

5

6

Fig. 3 Two CDK2 inhibitors with a donor and acceptor highlighted in each. The intrafeature distances are such that it is geometrically impossible to align the molecules with both features overlaid. Distance constraints are used to eliminate such unfeasible solutions from the population

Table 2 MOGA parameters

Parameter	Value
Selection pressure	1.05
Crossover rate	50%
Mutation rate	50%
Features niche radius	2
Volume overlap niche radius	100 Å^3
Energy niche radius	42 kJ mol^{-1}

Carbonic anhydrase dataset

The carbonic anhydrases are a family of enzymes which catalyse the conversion of water and carbon dioxide to bicarbonate and a proton. Inhibitors of carbonic anhydrase, particularly carbonic anhydrase II (CAII), have been successfully used to treat elevated intraocular pressure, the main cause of glaucoma [22]. The MOGA has been applied to a set of four inhibitors of human CAII, shown in Table 3. The true alignment of the ligands in the binding pocket was obtained by overlaying the protein structures using Relibase+ [23]. The interactions between the ligands and the protein were deduced by visual examination of the complexes and by referring to the literature references given for each entry in the PDB and are shown in Table 4. The features of the ligands have been labelled according to the interactions that they make with the protein.

The carbonic anhydrase binding site contains a zinc ion which is important to the mode of action of the enzyme [24]. Many carbonic anhydrase inhibitors, including all four in this dataset, coordinate to this zinc ion through a sulphonamide group [25]. Our program has not been specifically designed to characterise interactions with metal ions. However, the same types of functional group that are able to act as hydrogen bond acceptors tend to also coordinate to metal atoms. Therefore, the MOGA is able to generate pharmacophore points relating to the metal interactions, but gives these points acceptor type.

In view of its size, the butyl fragment in 1okm was treated as a hydrophobe. In fact, it forms hydrophobic

Table 3 CAII dataset

Molecule	PDB code	D1	A1	A2	A3	A4	H1	H2
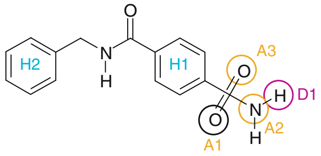	1g4o	✓	✓	✓	✓		✓	✓
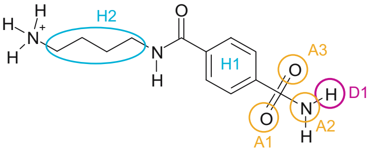	1okm	✓	✓	✓	✓		✓	✓
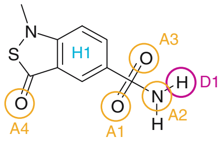	1kwr	✓	✓	✓	✓	✓	✓	
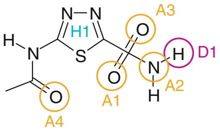	2h4n	✓	✓	✓	✓	✓	✓	

The interactions each ligand makes with the protein are shown

Table 4 The key interactions involved in binding to CAII

Type	Label	Interacting protein residue(s)
Donor	D1	THR199
Acceptor	A1	ZN262
	A2	ZN262
	A3	THR199
	A4	GLN92
Hydrophobe	H1	LEU198
	H2	PHE131, VAL135, PRO202, LEU204

interactions with the same protein residues as the terminal aromatic ring in 1g4o, and is very closely superimposed on that ring in the overlay of the crystal structures, as shown in Fig. 4a.

The interactions of the sulphonamide group and the adjacent hydrophobic ring are common to all four molecules, whereas the other interactions are present in only a subset of the dataset. When GASP is applied to this dataset, it consistently aligns the sulphonamide and H1 features correctly, and generates associated pharmacophore points. However, since there are no features in the other parts of the molecules that are common to the whole dataset, there is no incentive in terms of an improved fitness score for these parts of the molecules (such as the flexible tails of 1g4o and 1okm) to be aligned, and their relative conformations are arbitrary.

Figures 4b and c show typical solutions generated from a MOGA run with the CAII dataset. This run used a population size of 500 and was run for 200,000 operations, taking about 1 h. Three donor, six acceptor and two hydrophobe mapping columns were used in the chromosome. The other parameters were set as in Table 2. In both cases, it can be seen that the MOGA has correctly aligned the sulphonamide groups and H1 hydrophobic rings, and generated associated pharmacophore points. In overlay 4(b), a hydrophobic pharmacophore point has also been generated that corresponds to the partial match involving the aromatic H2 ring in 1g4o and the butyl hydrophobe in 1okm. In solution 4(c), a donor point has been generated that represents a partial match in 1g4o, 1okm and 2h4n. Solution 4(c), however, illustrates a limitation of our current method, since the H2 hydrophobic features have been overlaid but the mapping is not present within the mapping table so that no pharmacophore point has been generated. The diversity of the solutions produced for this dataset is limited due to the relatively small size and inflexibility of the ligands, however, slight differences are seen in the alignment and conformations of the two larger molecules.

Cyclin dependent kinase 2 datatset

The cyclin-dependent kinases are a class of proteins which play a vital role in the cell cycle, the mechanism by which eukaryotic cell division occurs [26]. Under

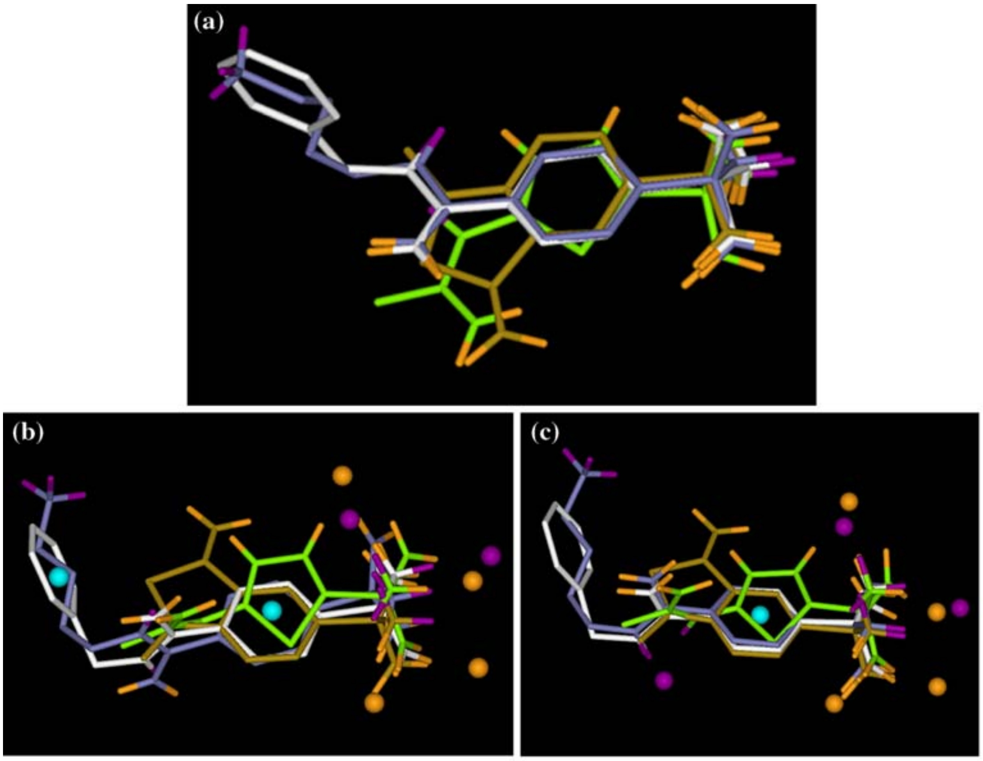

F = 2.10; V = 667 Å^3; E = –5.3 kJmol^{-1}

F = 2.31; V = 671 Å^3; E = –4.6 kJmol^{-1}

Fig. 4 The carbonic anhydrase dataset. 1g4o is white, 1okm is blue, 1kwr is brown and 2h4n is green. (**a**) PDB overlay of the CAII inhibitors; (**b**) and (**c**) show typical MOGA solutions together with their objective scores. Donors are highlighted in purple, acceptors in orange and hydrophobes in cyan

normal circumstances, cell cycle progression is highly regulated. Dysfunction of the normal regulatory processes is a critical feature of human cancers; therefore, the development of therapies which inhibit uncontrolled cell reproduction is currently an important area of pharmaceutical interest. Numerous crystal structures of complexes of ligands bound in the ATP binding pocket of Cyclin Dependent Kinase 2 (CDK2) are available in the PDB.

The ligands are shown in Table 5 and include some from the comparative study of pharmacophore generation programs carried out by Patel et al. [5]. As for the CAII dataset, the true alignment of the ligands in the binding pocket was obtained by overlaying the protein structures using Relibase+ [23] and the interactions between the ligands and the protein were deduced by visual inspection and by referring to the literature references given for each entry in the PDB. The features of the ligands have been labelled according to the interactions they make with the protein (Table 6), using the labelling scheme of Patel et al., which has been extended to include additional interactions not relevant to their dataset.

The CDK2 dataset is of interest in evaluating the identification of partial matches since several of the ligands, including the natural substrate, ATP, contain a purine ring system or another ring system of identical shape, but the ring systems adopt different alignments in different complexes. In the 2D diagrams in Table 5, the molecules are drawn so that their relative orientations correspond as closely as possible to the actual binding modes. Only three of the eight interactions are common to all seven molecule and even if the dataset is divided into subsets, there is only one pair of molecules (1ke5 and 1fvv) which form exactly the same set of interactions. Thus, it would not be easy to analyse this dataset using a pharmacophore program that is restricted to finding interactions that are present in all molecules.

The dataset was initially divided into two subsets as shown below, both of which involve the identification of partial matches. Finally the MOGA was run on the full dataset.

Subset 1: 1h1q, 1e1v, 1ckp

Molecules 1h1q, 1e1v and 1ckp were chosen for the initial experiment as they are relatively simple, but the purine rings bind in different orientations and all three molecules form interactions not common to the whole dataset. The overlay generated from the PDB structures is shown in Fig. 5a; the actual interactions formed with the protein are D2, A1 and H1 (by all molecules),

Table 5 CDK2 dataset

Molecule	PDB code	D1	D2	D3	A1	A2	H1	H2	H3
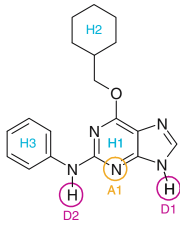 H2 O N H1 N H3 N H D2 N A1 N H D1	1h1q	✓	✓		✓		✓	✓	✓
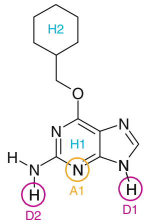 H2 O N H1 N H N H D2 N A1 N H D1	1e1v	✓	✓		✓		✓	✓	
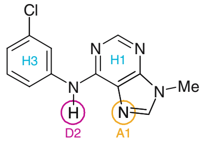	1ckp		✓		✓		✓		✓
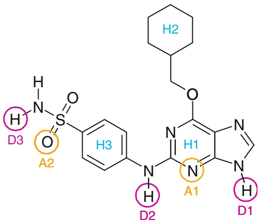 H2 H N O S H D3 O A2 H3 N H1 N N H D2 N A1 N H D1	1h1s	✓	✓	✓	✓	✓	✓	✓	✓
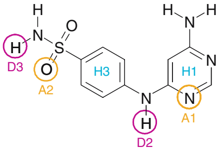 H N O S H D3 O A2 H3 H N H N H1 N H D2 N A1	1jsv		✓	✓	✓	✓	✓		✓
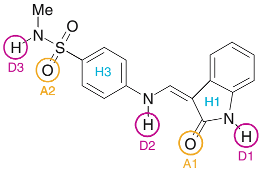 Me N O S H D3 O A2 H3 N H D2 H1 N O A1 H D1	1ke5	✓	✓	✓	✓	✓	✓		✓
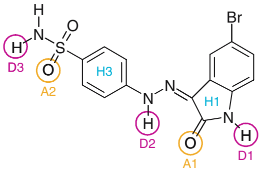 H N O S H D3 O A2 H3 Br N N H D2 H1 N O A1 H D1	1fvt	✓	✓	✓	✓	✓	✓		✓

The interactions that each ligand makes with the protein are shown

D1 and H2 (by 1h1q and 1e1v only), and H3 (by 1h1q and 1ckp only).

The MOGA was run with a population size of 1000 for 100,000 operations and took around 1.5 h. Two donor, one acceptor and three hydrophobe mapping columns were used in the chromosome. A representative set of solutions generated in a typical run, together with their objective scores, is shown in Figs. 5b–e. The MOGA consistently generated solutions very similar to the true overlay, such as that shown in Fig. 5b. This

Table 6 The key interactions involved in binding to CDK2

Type	Label	Interacting protein residue(s)
Donor	D1	GLU81
	D2	LEU83
	D3	ASP86
Acceptor	A1	LEU83
	A2	ASP86
Hydrophobe	H1	VAL18, ALA31, LEU134
	H2	VAL18, GLY11
	H3	ILE10, PHE82

solution contains six pharmacophore points (as many as are possible given the number of mapping columns used), three of which are common to all three molecules. The MOGA correctly identified the partial interactions D1 (present in 1h1q and 1e1v only), D2 (present in all three molecules) and H3 (present in 1h1q and 1ckp only). Two pharmacophore points were generated for interaction H1. This illustrates a further limitation of the current feature detection methodology, whereby each ring is treated as an individual hydrophobe so that fused ring systems cannot be

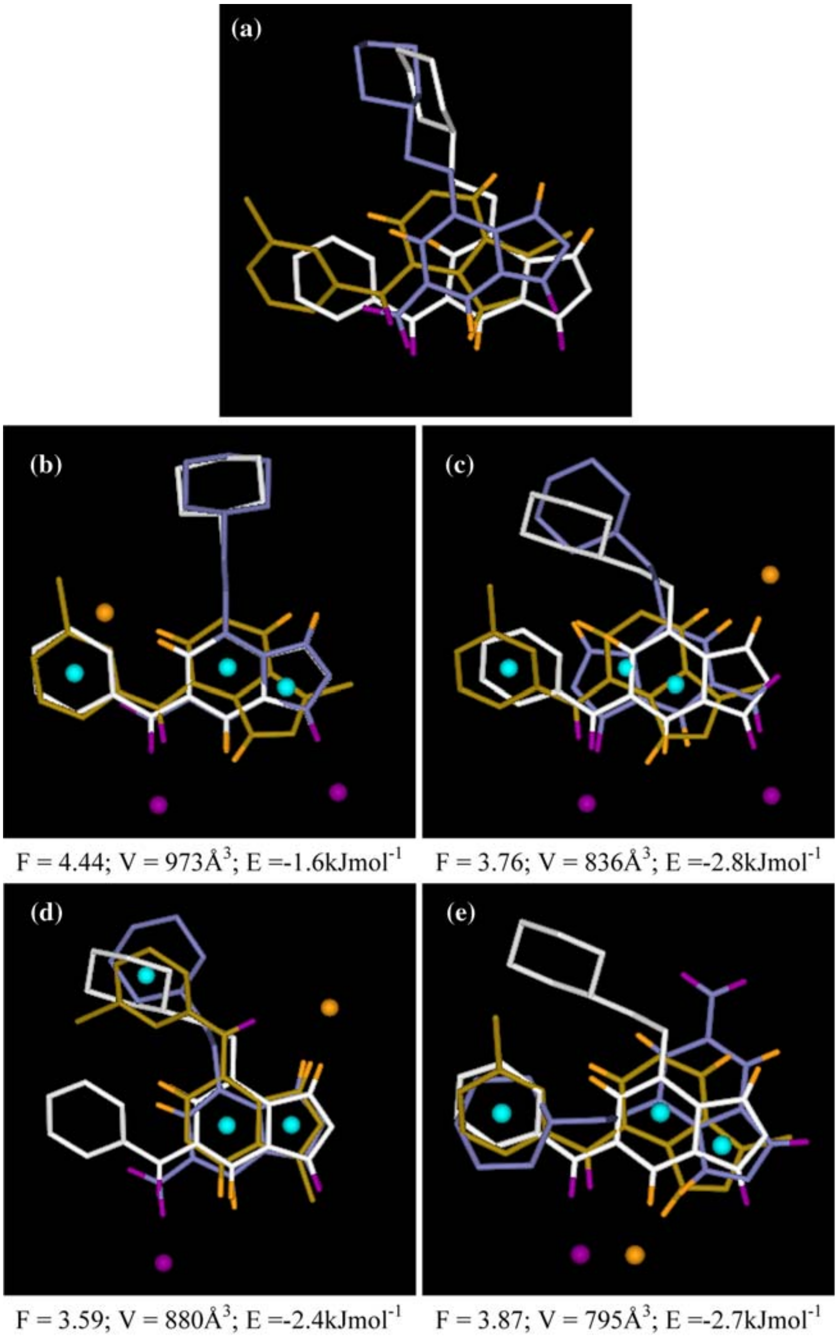
(a)
(b)
(c)
F = 4.44; V = 973Å^3; E =-1.6kJmol^{-1}
F = 3.76; V = 836Å^3; E =-2.8kJmol^{-1}
(d)
(e)
F = 3.59; V = 880Å^3; E =-2.4kJmol^{-1}
F = 3.87; V = 795Å^3; E =-2.7kJmol^{-1}

Fig. 5 CDK2 subset 1. 1h1q is white; 1e1v is blue; and 1ckp is brown. (**a**) The PDB overlay; (**b**)–(**e**) A typical set of solutions together with their objective scores generated for CDK2 subset 1. Donors are highlighted in purple, acceptors in orange and hydrophobes in cyan

recognised as a single hydrophobe. Although the cyclohexyl rings in 1h1q and 1e1v were overlaid, there were insufficient mapping columns to generate a point from these features as well as the two points generated for H1.

No pharmacophore point was generated in relation to interaction A1. Instead, the single acceptor mapping column was used to generate a point from a different set of nitrogen atoms on a different part of the ring systems. This illustrates a fundamental limitation of pharmacophore elucidation, which is not specific to our method, that if features of the same type are present at a common position in every molecule, then a pharmacophore point will generally be generated from these features, even if they do not actually make an interaction with the protein. In fact, the acceptors that have been mapped are slightly better aligned than the features that are overlaid in the true alignment, which partially explains why the MOGA generated a point from these features instead.

Other plausible solutions, such as those shown in Fig. 5c–e were also generated. Because 1h1q has an almost symmetrical arrangement of two donors and one acceptor, it was very common for 1e1v to be flipped relative to the true overlay, so that the opposite combination of donors is mapped between 1h1q and 1e1v. This is illustrated in overlay 5(c), which is otherwise fairly similar to the true overlay. Overlays 5(d) and 5(e) show two alternative overlays, in which the molecules are aligned such that a much larger volume is common to all three molecules. In both of these cases, four of the five pharmacophore points generated result from a mapping between all three molecules. Molecule 1ckp is flipped in solution 5(d) so that a hydrophobic feature is identified that is common to all three of the ligands and in solution 5(e) molecule 1e1v is flipped.

Subset 2: 1h1s, 1jsv, 1ke5, 1fvt

1h1s is identical to 1h1q except for the addition of a sulphonamide group on the benzene ring, and it makes the same interactions as 1h1q, together with additional interactions via the sulphonamide group. In fact, the presence of the sulphonamide group leads to a 150-fold greater affinity of 1h1s relative to 1h1q, due to the formation of hydrogen bonds by one of the sulphonamide hydrogens and one of the oxygens to the ASP86 residue of the protein [27]. All of the other molecules in this subset also possess sulphonamide groups which overlay very closely on the sulphonamide group of 1h1s, as shown in the PDB overlay in Fig. 6a. The common interactions formed by this subset are D2, D3, A1, A2, H1 and H3 (all molecules) and D1 (1h1s, 1ke5 and 1fvt only).

The MOGA was run with a population size of 1000 for 100,000 operations and took around 1.4 h. Four donors, five acceptors and two hydrophobe mapping columns were used in the chromosome, to allow for the possibility of mapping multiple features within the sulphonamide groups. Almost all of the solutions generated by the MOGA comprised approximately the same alignment as the true overlay. However, two solutions showing some variation in the exact alignment are shown in Figs. 6b and c. The correct interactions have mostly been identified. However, there is no pharmacophore point relating to interaction H1. As discussed for the CAII dataset, a limitation of the current method is that features can be overlaid even though they are not included in the mapping encoded in the chromosome, and hence they do not result in the generation of a pharmacophore point. Similarly, where several features are overlaid, it is possible that only a subset of these features is mapped. In this case, a pharmacophore point would be generated, but its feature score would be based only on the features that are mapped. Hence, the score would be smaller than if all the features were mapped. This explains the relatively low feature score of these solutions.

Pharmacophore points have been identified within the sulphonamide groups; however, the MOGA cannot be expected to correctly identify the rotation of the sulphonamide groups relative to the adjacent aromatic rings, since any rotation consistently applied to each molecule would lead to an overlay of the features. Although only one of the sulphonamide hydrogens and one lone pair actually makes an interaction with the protein, the other hydrogens and lone pairs are still overlaid. Therefore, the MOGA has generated additional points related to the sulphonamide features.

Full dataset

The MOGA was applied to the full set of molecules, excluding 1fvt which was not included since it is identical to 1ke5 apart from the addition of a bromine atom. Distance constraints were derived following a systematic search and were used to reduce the search space explored by the MOGA.

The MOGA was run with a population size of 2000 for 200,000 operations, five donor, six acceptor and three hydrophobe columns were specified and the run took around 15 h. The population size and number of

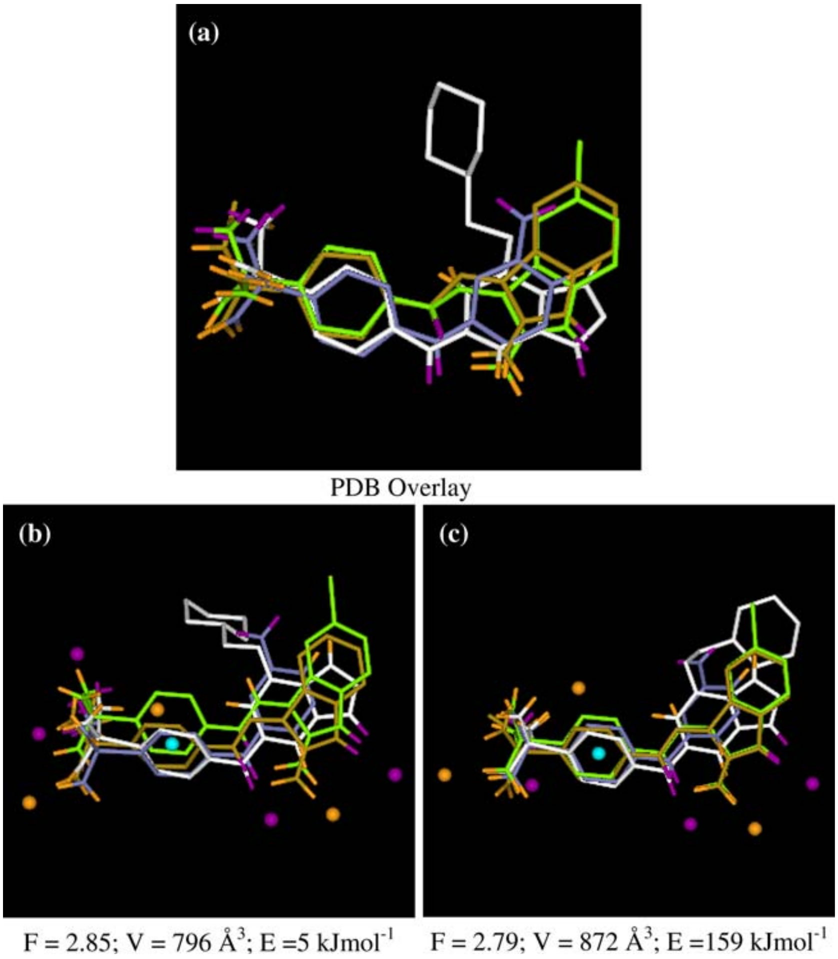

PDB Overlay

F = 2.85; V = 796 Å^3; E =5 kJmol^{-1}

F = 2.79; V = 872 Å^3; E =159 kJmol^{-1}

Fig. 6 CDK2 subset 2. (**a**) the PDB overlay. (**b**) and (**c**) show example solutions together with their objective scores. Donors are highlighted in purple, acceptors in orange and hydrophobes in cyan

operations were increased due to the increase in search space for this larger set of feature rich molecules. The true overlay is shown in Fig. 7a and a MOGA solution that is close to the PDB-derived solution is shown in Fig. 7b. All of the molecules except 1ke5 are aligned approximately correctly. However, 1ke5 is flipped relative to the true overlay so that its sulphonamide group is facing in the opposite direction to those of 1h1s and 1jsv. In fact, the true overlay does not show a particularly close alignment of 1ke5 to the other molecules. Although the alignment shown does not enable the sulphonamide group of 1ke5 to map to the other sulphonamides, the contribution of any potential sulphonamide mappings to the total feature score must be small because they can involve at most three out of the six molecules. Any potential improvement in the feature score that would result from mapping the three sulphonamide groups is probably outweighed by the closer alignment of the molecular backbones compared to the true overlay.

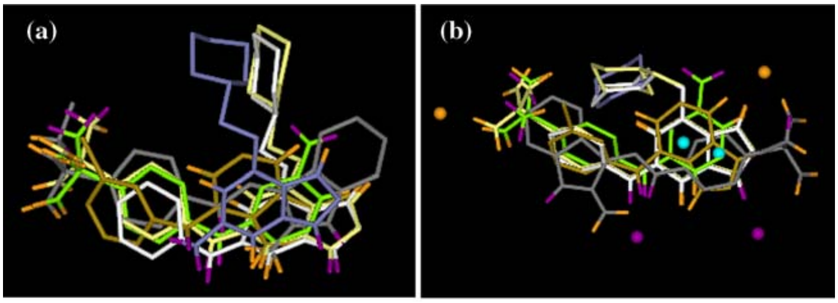

F = 1.66; V = 942 Å^3; E =101 kJmol^{-1}

Fig. 7 The full CDK2 dataset. 1h1q is shown in white, 1e1v in blue, 1ckp in brown, 1h1s in yellow, 1jsv in green and 1ke5 in grey. (**a**) The PDB overlay and (**b**) an overlay generated by the MOGA. Donors are highlighted in purple, acceptors in orange and hydrophobes in cyan

Conclusions

The paper has described the extension of our earlier work [9] to incorporate partial matches within a multiobjective optimisation approach to pharmacophore identification. Pharmacophore methods are particularly useful if they can be applied to datasets of structurally diverse molecules, where they may be able to suggest overlays that are not obvious to the chemist. However, diverse sets of molecules rarely adopt exactly the same binding mode. Hence, programs that make the assumption of a common binding mode are not able to handle diverse datasets effectively. Allowing the identification of partial matches removes the restriction that every molecule must match every pharmacophore point, which allows the program to be applied to larger and more diverse datasets.

The datasets investigated here were extracted from the PDB so that the true solution is known and hence the program can be validated. However, pharmacophore identification is typically used when structural information on the binding site is unavailable and in the absence of such data, it is unlikely that a single solution could be predicted unambiguously. Incorporating the improved functionality within a multiobjective framework results in the identification of a family of plausible solutions where each solution represents a different overlay involving different mappings between the molecules, and where the solutions taken together explore a range of different compromises in the objectives. The solutions are not ranked but are presented as equally valid compromises between three objectives, according to the principles of Pareto dominance. Importantly, the MOGA also takes into account the chemical diversity of the solutions, thus ensuring that the solutions represent a diverse range of structure-activity hypotheses which could be presented to a medicinal chemist for further consideration. In cases where a large number of plausible hypotheses exist it would be beneficial to provide the user with a browsing tool to facilitate navigation through the different possibilities. Such a tool might incorporate clustering techniques similar to the mapping-based clustering which is applied during the search process itself or clustering based on geometric criteria.

The presence of partial matches also has implications on how such a pharmacophore hypothesis would be used in database searching since it represents the union of the set of features common to each pair of molecules. While a molecule which matches every feature in the set is likely to be active, the hypothesis represents an over-restrictive specification of the requirements for activity, since many or all of the known active molecules possess only a subset of the features. Hence, when performing pharmacophore-based virtual screening using a query generated with the partial matching methodology, it would be useful to allow the identification of molecules which match only a subset of the points in the query. The hits would then be likely to contain molecules representing a range of binding modes, and the plausibility of each of these could then be evaluated visually or experimentally by the user.

A number of areas for further improvement have been identified and are currently under investigation. For example, as discussed, the implementation of the partial match methodology required the development of a new alignment method whereby the molecules are aligned sequentially to a common framework. When a molecule is incorporated into the framework, the framework is adjusted to take account of all molecules already aligned. However, the alignment method currently implemented is dependent on the order in which the molecules are specified in the configuration file. Future work will investigate the implementation of an order-independent method for the multiple-molecule alignment with several methods having been described in the literature [19, 28–30], Similarly, the volume objective function is order dependent which is also unsatisfactory, since volumes that are common to most of the molecules but not the first molecule currently make no contribution to the volume score. Thus, we are focussing on taking into account any volume that is occupied by two or more molecules, but with the contribution from each point in space weighted so that points occupied by more molecules make a larger contribution to the overall score.

References

1. Güner OF (ed) (2000) Pharmacophore perception, development and use in drug design. International University Line, La Jolla, CA
2. Jones G, Willett P, Glen RC (1995) J Comput Aided Mol Des 9:532
3. Barnum D, Greene J, Smellie A, Sprague P (1996) J Chem Inf Comput Sci 36:563
4. Martin YC, Bures MG, Danaher EA, Delazzer J, Lico I, Pavlik PA (1993) J Comput Aided Mol Des 7:83
5. Patel Y, Gillet VJ, Bravi G, Leach AR (2002) J Comput Aided Mol Des 16:653
6. van Drie JH (2003) Curr Pharm Design 9:1649
7. Richmond NJ, Willett P, Clark RD (2004) J Mol Graphics Model 23:199
8. Feng J, Sanil A, Young SS (2006) J Chem Inf Model 46:1352
9. Cottrell SJ, Gillet VJ, Taylor R, Wilton DJ (2004) J Comput Aided Mol Des 18:665
10. Galahad. Tripos Inc. (1699) South Hanley Rd, St. Louis, Missouri, 63144, USA

11. Goldberg DE (1989) Genetic algorithms in search, optimization and machine learning. Wokingham, Addison-Wesley
12. Fonseca CM, Fleming PJ (1998) IEEE Trans Syst Man Cybern A – Syst Humans 28:26
13. Handschuh S, Wagener M, Gasteiger J (1998) J Chem Inf Comput Sci 32:220
14. Gillet VJ, Khatib W, Willett P, Fleming PJ, Green DVS (2002) J Chem Inf Comput Sci 42:375
15. Nicolotti O, Gillet VJ, Fleming PJ, Green DVS (2002) J Med Chem 45:5069
16. Brown N, McKay B, Gasteiger J (2004) J Comput Aided Mol Des 18:761
17. Catalyst. Accelrys, 9685 Scranton Road, San Diego, CA 92121, USA
18. Berman HM, Battistuz T, Bhat TN, Blum WF, Bourne PE, Burkhardt K, Feng Z, Gilliland GL, Iype L, Jain S, Fagan P, Marvin J, Padilla D, Ravichandran V, Schneider B, Thanki N, Weissig H, Westbrook JD, Zardecki C (2002) Acta Crystallogr D58:899
19. Sutcliffe MJ, Haneef I, Carney D, Blundell TL (1987) Protein Eng 1:377
20. Kabsch W (1976) Acta Crystallogr A 32:922
21. Raymond JW, Willett P (2003) J Chem Inf Comput Sci 43:908
22. Supuran CT, Scozzafava A (2002) Expert Opin Therapeut Patents 12:217
23. Hendlich M, Bergner A, Gunther J, Klebe G (2003) J Mol Biol 326:607
24. Tu CK, Silverman DN, Forsman C, Jonsson BH, Lindskog S (1989) Biochemistry 28:7913
25. Abbate F, Supuran CT, Scozzafava A, Orioli P, Stubbs MT, Klebe G (2002) J Med Chem 45:3583
26. Sielecki TM, Boylan JF, Benfield PA, Trainor GL (2000) J Med Chem 43:1
27. Davies TG, Bentley J, Arris CE, Boyle FT, Curtin NJ, Endicott JA, Gibson AE, Golding BT, Griffin RJ, Hardcastle IR, Jewsbury P, Johnson LN, Mesguiche V, Newell DR, Noble MEM, Tucker JA, Wang L, Whitfield H (2002) J Nat Struct Biol 9:745
28. Mestres J, Rohrer DC, Maggiora GM (1997) J Comput Chem 18:934
29. Gerber PR, Muller K (1987) Acta Crystallogr A 43:426
30. Kearsley SK (1990) J Comput Chem 11:1187